Dynamics of a Near-Resonant Fluid-Filled Gyroscope

Roger F. Gans*
U. S. Army Ballistic Research Laboratory, Aberdeen Proving Ground, Maryland

The behavior of a fluid-filled gyroscope having a natural coning frequency near that of the inertial oscillation of a contained rotating liquid is calculated. The limitations of the calculations are that the coning angle be small enough to make the linearization of the Navier-Stokes equations appropriate and that the liquid viscosity be low enough to make boundary-layer techniques appropriate. The theory is compared to observations from the literature to assess the limitations of the theory. Some comparison with earlier work is given. It is concluded that the present theory reflects the data reasonably well and that it is an improvement over previous work.

I. Introduction

SPINNING fluid-filled containers (examples include fluid-filled artillery shells and spacecraft with liquid-fueled apogee engines) can be unstable to growing pitch and yaw. For successful flight, the angle between the spin axis and the flight path (herein called the coning angle) must remain small. The motion of the container axis forces differential motions within the fluid, which in turn produce torques on the container. If the torques are such as to increase the coning angle, the container can be unstable. Coning at a frequency at or near an inertial mode frequency of the rotating liquid leads to a resonant liquid response and much larger torques.

A flying container is acted on by many forces and torques other than the fluid dynamical ones that form the main topic of this paper. Attention will be restricted to fluid-filled gyroscopes, which cone freely in the laboratory. The coning angle grows with time; and this growth rate is determined almost entirely by the response of the contained fluid to the coning motion. Since the initial coning angle is essentially zero, the Navier-Stokes equations can be linearized about a solid rotation using the coning angle as the small parameter. previous work addressing the fluid dynamics includes that of Gans,[1] which was specifically designed to deal with the resonance for forced coning, Murphy,[2] and Gerber et al.[3,4] The present work is an extension of Ref. 1. The Murphy work contains a comprehensive bibliography of the literature, especially that of the projectile community. The differences between Refs. 3 and 4 and the present work are discussed in the final section.

The motion of a gyroscope can be described in terms of the motion of its symmetry axis. The axis can be described instantaneously in an inertial system in which it is initially vertical by a unit vector

$$\boldsymbol{K}=\sin\alpha\cos\Omega t\boldsymbol{i}_I+\sin\Omega t\boldsymbol{j}_I+\cos\alpha\boldsymbol{k}_I \tag{1}$$

where $\boldsymbol{i}_I$, $\boldsymbol{j}_I$, and $\boldsymbol{k}_I$ denote inertial Cartesian unit vectors. Both α and Ω can be *slowly varying* functions of time. This will be discussed in greater detail in Sec. III.

An inertial system is not convenient for either the gyroscope dynamics or the fluid dynamics. Two noninertial coordinate systems will be introduced. In both of these, the unit vector $\boldsymbol{k}$ is parallel to $\boldsymbol{K}$.

The first coordinate system, denoted by a subscript I, is useful for gyroscope dynamics. In this coordinate system, the projections of the unit vectors $\boldsymbol{i}_I$ and $\boldsymbol{j}_I$ onto the inertial x,y plane are always in the $\boldsymbol{i}_I$ and $\boldsymbol{j}_I$ directions, respectively.

The second system, denoted by a subscript 2, has an additional rotation about the $\boldsymbol{k}_I$ (coning) axis. This rotation fixes $\boldsymbol{k}_I$ in the second noninertial system. This system is the same as that used in Ref. 1 and can be called the coning system. In this system, both the axis of the gyroscope $\boldsymbol{K}$ and the axis about which $\boldsymbol{K}$ cones appear fixed. It is the system of an observer who moves with the gyroscope axis, but who does not spin—that is, an observer who is on the gimbals.

The x and y components of the two systems are connected by their x and y unit vectors

$$\boldsymbol{i}_I=\cos\Omega t\boldsymbol{i}_2-\sin\Omega t\boldsymbol{j}_2$$

$$\boldsymbol{j}_I=\sin\Omega t\boldsymbol{i}_2+\cos\Omega t\boldsymbol{j}_2 \tag{2}$$

Suppress the subscript I as redundant for the rest of this section, and let I_z and I_x denote the total axial and transverse moments of inertia of the liquid container system (including the mass of the liquid, viewed as a rigid body). Let the coordinate system pitch at the rate $\omega\theta'$ about the $\boldsymbol{j}$ axis snd yaw at a rate $\omega\psi'$ about the $\boldsymbol{i}$ axis. (Coning, of course, is pitching and yawing at frequency Ω, 90 deg out of phase.) Let the container also rotate at angular velocity $\omega\phi'$ about the $\boldsymbol{k}$ axis. Here ω is the spin rate of a driven gyroscope. For a general vehicle, it would represent some mean spin. The problem will be nondimensionalized, time being measured in units of ω^{-1}, length in units of the cavity radius a, and inertia in units of I_x. Thus, the prime denotes the derivative with respect to ωt.

For the remainder of this paper, t will be used to denote the dimensionless time.

Let the fluid velocity to be solid corotation with its container, plus whatever perturbation flow is driven by the coning. (This is consistent with the definition of the moments of inertia to include the fluid mass.) Denote the deviation flow by $\omega a\boldsymbol{v}$.

The total angular momentum in this coordinate system may be written as

$$\boldsymbol{J}=\omega I_x[\psi'\boldsymbol{i}+\theta'\boldsymbol{j}+\sigma\phi'\boldsymbol{k}]+\boldsymbol{\Gamma} \tag{3}$$

where $\boldsymbol{\Gamma}=\rho\omega a^2\langle\langle\boldsymbol{r}\times\boldsymbol{v}\rangle\rangle$, ρ denotes the liquid density, $\sigma=I_z/I_x$, and the double angle bracket notation denotes the integral over the volume of the liquid.

The dynamical equations are obtained by equating the rate of change of the angular momentum to the applied torque.

Received March 11, 1983; revision received Dec. 22, 1983.

*Associate Professor of Mechanical Engineering, University of Rochester, Rochester, N.Y. (on leave).

After completing the nondimensionalization, these become

$$M_x=\psi''+\sigma\theta'\phi'+\epsilon(\alpha\tau G_x)'$$
$$M_y=\theta''-\sigma\psi'\phi'+\epsilon(\alpha\tau G_y)' \quad (4)$$
$$M_z=\sigma\phi''+\epsilon\alpha(\psi' G_y-\theta' G_x)$$

where the external torque $T=I_x\omega^2 M$, $\epsilon=m_L a^2/I_x$, $\tau=\Omega/\omega$, m_L denotes the liquid mass, and

$$\Gamma=m_L a^2\Omega\alpha G \quad (5)$$

Equations (4) are nonlinear, but they can be reduced to a sequence of linear equations when α is small. For the gyroscope problem under consideration, the first of these determines τ and the second the rate of change of α. The details are given in Sec. III.

The explicit appearance of Ω and α in Eq. (5) anticipates the fluid dynamical result that ν (and hence Γ) is proportional to both τ (and hence Ω) and α.

II. The Fluid Dynamical Problem

The second coordinate system will be used exclusively in this section and the subscript *2* will be suppressed. The discussion is dimensionless.

The fluid dynamical and coning problems are coupled. One should solve the fluid dynamical problem keeping ψ, ϕ, and θ as functions of time. In principle, this can be done but the complications are formidable. The essentials of the physics is revealed by a quasistatic analysis in which it is supposed that the fluid responds "instantaneously" to changes in the basic parameters. Since the response time of a rotating viscous fluid is of the order $L/(\omega\nu)^{1/2}$ for a container with a characteristic length L rotating at ω and containing a fluid with kinematic viscosity ν, changes in the dynamical parameters should be slow compared to that time.

Let the cavity described above contain an incompressible fluid with a kinematic viscosity ν. Denote the (dimensionless) cylindrical coordinates by r, ϕ, and z. In this system the container motion is steady solid rotation about its principal axis at the unit angular frequency. The coning vector is parallel to the mean gyroscope axis (or the flight path in the case of an actual vehicle). The fluid velocity q is decomposed (in the coning system) as

$$q=k\times r+\alpha u \quad (6)$$

[Note that this decomposition is *not* a coordinate transformation. The flow has merely been divided into a component satisfying the no-slip boundary conditions and a component u $(=\nu/\alpha)$ satisfying the homogeneous (zero) boundary conditions.]

The substitution of this representation of q into the Navier-Stokes equations introduces an inhomogeneous term into the momentum equations. That term is singly periodic in the azimuthal angle, suggesting the introduction of complex notation. Let

$$\cos\phi=e^{i\phi}/2+\text{cc}; \quad 2u=Ue^{i\phi}+\text{cc}, \quad 2p=Pe^{i\phi}+\text{cc} \quad (7)$$

where cc is complex conjugate and U and P are functions of r and z only. Subsequent linearization based on the smallness of the angle α leads to the following equations for U and P:

$$isU+2k\times U+\nabla P=E\nabla^2 U-2fkr, \quad \text{div}(U)+iV/r=0 \quad (8)$$

where $s=1/(1+\tau)$, $f=\tau s$, $E=\nu/[\omega a^2(1+\tau)]$ is the Ekman number, and ∇P is shorthand for $e^{-i\phi}\nabla(2p)$.

The equations as they stand are not tractable analytically. Fortunately, in most applications $E\ll 1$ and a boundary-layer analysis is appropriate. One can divide the flow U into interior and boundary-layer components $\hat{U}$ and $\tilde{U}$, respectively. The former satisfies the governing equations in the limit that $E=0$ and the boundary conditions on the velocity normal to the wall. The latter varies rapidly in the direction normal to the wall (so that the viscous term is retained in the equations through the second derivative in the normal direction). It also satisfies the tangential no-slip boundary conditions.

The inviscid equations of motion can be obtained from the general set by letting $E=0$. The velocity components U, V, and W can be eliminated in favor of P. Subsequent substitution into the second of Eq. (8) leads to the Poincaré equation

$$\frac{1}{r}\frac{\partial}{\partial r}\left(r\frac{\partial P}{\partial r}\right)-\frac{1}{r^2}P-X^2\frac{\partial^2 P}{\partial z^2}=0 \quad (9)$$

where $X^2=(4-s^2)/s^2$. This equation is to be solved subject to the radial boundary condition $U=0$, which can be written in terms of P as

$$s\frac{\partial P}{\partial r}+2P=0 \text{ at } r=1 \quad (10)$$

The condition that $W=0$ on $z=\pm c/a$ becomes $\partial P/\partial z=-2fr$.

Solutions of Eqs. (9) and (10) can be written in terms of the eigenfunctions $P_m=J_1(j_m r)\cos k_m z$, where the parameter j_m is an eigenvalue determined by Eq. (10) and Eq. (9) determines the relationship between j and k: $j^2=X^2k^2$. The axial boundary condition is inhomogeneous, so that it determines the amplitude to be associated with each eigenfunction [after expanding r in a Dini series[5] in $J_1(j_m r)$].

If $\cos(k_m c/a)=0$ for any m, the amplitude of the mth mode is formally infinite and the system is said to resonate. Let n denote the value of m for which this happens and let $A_n=A$.

An alternative method for calculating the amplitude of this mode is necessary [as well as an alternate method of satisfying the inhomogeneous boundary condition on the end walls, because the Dini expansion for r will still contain a term proportional to $J_1(j_n r)$]. The amplitude must depend on the physics that has been neglected. In a linear analysis, a viscous balance is appropriate and will be sought. (The viscous amplitude relation turns out to be closely related to the "viscous correction" to the resonant frequency. The amplitude determined can be shown to be equivalent, to lowest order, to that found using Wedemeyer's method of corrected boundary position.[6])

Let the resonant pressure and velocity be $P^{(0)}$ and $U^{(0)}$, equal to $\tau A P_H$ and $\tau A U_H$, where $P_H=P_n$, the resonant eigenfunction. The remainder of the solution will be denoted by $P^{(1)}$ and $U^{(1)}$. A is determined by constructing a solvability condition for the problem determining $P^{(1)}$: that the resonant mode be orthogonal to the inhomogeneities. Manipulation of the orthogonality condition reduces it to a balance between the amplitude of the forcing and the "Ekman suction" associated with the resonant mode. Since the latter involves the amplitude of the resonant mode, the only undetermined quantity, this balance determines the amplitude of the resonant mode.

Strictly speaking resonance is defined only for $s=s_{cr}$, but, since the equations are analytic in s, the solutions should be near resonance when s is near s_{cr}. To include that possibility, let

$$s=s_{cr}+E^{1/2}s^{(1)} \quad (11)$$

where $s^{(1)}=\mathcal{O}(1)$. (This anticipates the result that the viscous correction will be $\mathcal{O}(E^{1/2})$ smaller than the leading term of the solution.) Similarly the velocity (and pressure) is expanded as

$$U=\tau A U_H+\tau U^{(1)}+\ldots \quad (12)$$

The two problems to be solved, in succession, can be written

$$is_{cr}U_H+2k\times U_H+\nabla P_H=0;\qquad \nabla\cdot U_H+iV_H/r=0 \quad (13a)$$

with

$$n\cdot U_H=0 \quad (13b)$$

on the boundary, and

$$is_{cr}U^{(1)}+2k\times U^{(1)}+\nabla P^{(1)}=-2s_{cr}rk-is^{(1)}E^{1/2}AU_H$$

$$\mathrm{div}(U^{(1)})+iV^{(1)}/r=0 \quad (14a)$$

with

$$n\cdot U^{(1)}=-n\cdot A\tilde{U}_H \quad (14b)$$

on the boundary. $\tilde{U}_H$ denotes the efflux associated with the boundary-layer corrections to the homogeneous solution. (See the Appendix for details of the boundary-layer solution.)

Multiply the conjugate of the first set by $U^{(1)}$ and the second by U_H^*, integrate over the volume of the cylinder, and add the results. The time derivative (is) terms and the Coriolis terms cancel. The divergence condition can be used to transform the pressure gradient integrals into surface integrals and the boundary conditions can be used to simplify those. The result is a single equation for A,

$$A[\langle P_H^* n\cdot\tilde{U}_H\rangle - is^{(1)}E^{1/2}\langle\langle U_H\cdot U_H^*\rangle\rangle]=s_{cr}\langle\langle rW_H^*\rangle\rangle \quad (15)$$

where $\langle\ldots\rangle$ denotes the integral over the container surface, $\langle\langle\ldots\rangle\rangle$ the integral over the volume, and the asterisk the complex conjugate.

Substitution of the actual eigenmodes and some calculation gives the following explicit expression for A:

$$A=i8(2/E)^{1/2}s(2+s)\sin(kc/a)/[Xk^2(1+k^2)JD(1+\tau)] \quad (16)$$

where $J=J_1(j)$ and

$$D=(S^+-iS^-)\sin^2(kc/a)+2s^{3/2}X(c/a)(1+i)$$
$$+i4\sqrt{2}(c/a)[2-s/(1+k^2)]s^{(1)}/Xs \quad (17)$$

and

$$S^+=(2+s)^{3/2}+(2-s)^{3/2};\qquad S^-=(2+s)^{3/2}-(2-s)^{3/2} \quad (18)$$

Note that $\sin(kc/a)=\pm 1$.

The three terms in D represent endwall boundary-layer flux, sidewall boundary-layer flux, and the departure from inviscid resonance, respectively.

The nonresonant solution is usually not explicitly calculated in problems of this type. However, it is needed for numerical results. The pressure $P^{(1)}$ is given by

$$P^{(1)}=c_1J_1(jr)z\cos kz+c_2rJ_2(jr)\sin kz+\sum_{m\neq n}A_mP_m(r,z) \quad (19)$$

where the constants A_m, c_1, and c_2 are determined from the boundary conditions.

The coefficients A_m can be found from the nonresonant part of the boundary conditions,

$$A_m=-4Fs/[(2-s)(1+k_m^2)J_1(j_m)\cos(k_mc/a)] \quad (20)$$

The resonant boundary conditions determine c_1 and c_2 in terms of A. These are that $U+A\tilde{U}_H$ must vanish on $r=1$ and that $W+A\tilde{W}_H$ must vanish on $z=\pm c/a$, and they give

$$c_1=2s\langle r\rangle_n/[(kc/a)\sin(kc/a)]$$
$$+ik^2A(S^+-iS^-)(E/2)^{1/2}/[2s^2Xkc/a]$$
$$c_2=E^{1/2}[2ks^{(1)}/(1+k^2)-(1-i)k(Xs)^2(2s)^{-1/2}]/(s^2X)A \quad (21)$$

where

$$\langle r\rangle_n=2s/[(2-s)(1+k^2)J_1(j)]$$

is the "resonant term" in the Dini expansion of r. Note that c_1 and c_2 are $\mathcal{O}(s,AE^{1/2})=\mathcal{O}(1)$, as they must be.

The differential equation imposes a third condition on c_1 and c_2

$$X^2kc_1+jc_2=4k^2AE^{1/2}s^{(1)}/s^3 \quad (22)$$

This provides an alternate method for the calculation of A. The A determined this way is the same as that determined by the integral method. [Factors of $\sin(kc/a)$ appear in different places, but the overall expressions are equivalent when $\sin(kc/a)=\pm 1$.]

III. System Dynamics

The quantity G defined in Sec. I can be written in the second coordinate system as

$$G=G_1i_2+G_2j_2 \quad (23)$$

and manipulation of the solution in Sec. II leads to a complex representation of G,

$$i(G_1-iG_2)=\int dr r\int dz[z(U-iV)-rW] \quad (24)$$

where the r integral is carried out from 0 to 1 and the z integral from $-c/a$ to c/a.

Substitution of the solution given above and carrying out of the integration gives

$$G_1-iG_2=-2J\sin(kc/a)A/[k^2(2-s)]$$
$$\times\{2-2(s-1)E^{1/2}s^{(1)}/(sk)$$
$$+[(kc/a)^2-2](c_1/k)+[2+5s-(2-s)k^2][c_2/(sj)]\}$$
$$+E^{1/2}J\sin(kc/a)(1-i)[(c/a)(2-s)^{-3/2}-(2/s)^{3/2}(1+k^2)/(2k^2)]A$$
$$-2/(2-s)\Sigma A_mJ_1(j_m)[2\sin(k_mc/a)-(k_mc/a)\cos(k_mc/a)]/k_m^2$$
$$-[(4c)/(3a)] \quad (25)$$

Each line of this expression represents a different contribution. In order, these are: the interior contribution from the resonant mode plus the interior contribution from the imperfect resonant match, the interior contribution from the correction to the resonant mode, the boundary layer associated with the resonant mode, the nonresonant interior solution, and the forcing term.

The transformation from x_2 to x_1 coordinates gives

$$G_x=G_1\cos\tau t-G_2\sin\tau t,\qquad G_y=G_1\sin\tau t+G_2\cos\tau t \quad (26)$$

and the dimensionless dynamical equations become

$$M_x=\psi''+\sigma\theta'\phi'-\epsilon\tau[\alpha\tau G_y-\alpha' G_x]+\ldots \quad (27a)$$

$$M_y=\theta''-\sigma\psi'\phi'+\epsilon\tau[\alpha\tau G_x+\alpha' G_y]+\ldots \quad (27b)$$

$$M_z = \sigma\phi'' - \epsilon\alpha[(\psi' G_1 + \theta' G_2)\sin\tau t + (\theta' G_1 - \psi' G_2)\cos\tau t] \tag{27c}$$

The omitted terms involve derivatives of Ω, G_1, and G_2.

The angles θ and ψ oscillate about their mean positions with an amplitude α. From the third equation, the variation in ϕ', in the absence of external torques, is at most of $\mathcal{O}(\alpha^2)$, and hence will be negligible in the dynamics. Thus, in the absence of external torques, ϕ' can be taken to be unity. When external torques are present, there will be a term linear in t in the x and y torque equations.

Solutions of the form

$$\psi = \alpha\cos\tau t, \quad \theta = \theta_0 - \alpha\sin\tau t, \quad \phi = \phi_0 + \phi' t \tag{28}$$

will be sought, where, in general, α and τ will be functions of time. For free gyroscope experiments ϕ' is constant (held so by a drive motor), $M_x = 0 = M_y$ (neglecting bearing friction, of which more later), and the equations admit solutions with constant τ and

$$\alpha = \alpha_0 \exp(\lambda\tau t) \tag{29}$$

Substitution of this hypothesis into the differential equations and subsequent neglect of the omitted terms in Eqs. (28a) and (28b) leads to expressions that can be solved for λ and τ,

$$[(1-\lambda^2) + \epsilon G_1]\tau - [\sigma + \epsilon\tau\lambda G_1] = 0$$

$$[2\tau - \sigma - \epsilon\tau G_2]\lambda = -\epsilon\tau G_2 \tag{30}$$

Typically, ϵ is small (the container is more massive than the liquid), λ must be small for the analysis to apply, and one can write,

$$\tau \approx \sigma/[1 + \epsilon G_1], \quad \lambda \approx -\epsilon\tau G_2/[2\tau - \sigma] \tag{31}$$

IV. Comparison with Other Models and with Experiment

Before examining the experimental data, it is useful to discuss briefly the other models available.[2-4] These models differ from the present one in both principle and detail. The important difference is in the method of determining the resonant frequency.

The resonant frequency is measured in the coning system. One wants to know its relation to the excitation (coning) frequency τ. Let the critical frequency be s_{cr}. It is related to the critical coning frequency τ_{cr} by

$$s_{cr} = 1/(1 + \tau_{cr}) \tag{32}$$

In the work cited above the analogous relation has been

$$s_{cr} = 1 - \tau_{cr} \tag{33}$$

The difference arises from the choice of coordinate system. In the present work the system cones, but in the previous work it does not. [See the development leading to Eq. (8)]. The difference is clearly reflected in the behavior of the solution as $\alpha \to 0$. Imagine a cylinder rotating about its symmetry axis at ω. Let that symmetry axis rotate at Ω about an axis inclined at the small angle α. [Imagine the container and its spin motor on a rotating table at an angle α from the (vertical) table rotation axis.]

In the limit that $\alpha \to 0$, one should obtain the basic unperturbed state. For the thought experiment just described, the state is solid rotation about the container symmetry axis *at the combined rotation rate*, $\omega + \Omega$. Previous formulations produce solid rotation at the rotation frequency ω. This is equivalent to the small parameter being the product $\tau\alpha$. (See also Greenspan.[7])

Thus the previous work cited has been constructed assuming that the basic state was that of solid rotation at the container frequency in an unyawed orientation. The s,τ relation appropriate to the basic state is $s = 1 - \tau$. However, because the basic expansion parameter associated with that basic state is not α, but $\tau\alpha$, it is likely that the results may be less accurate when compared to experiment than those from a less restrictive expansion. This point will be explained further.

The two different formulations agree where they overlap, because $1/(1+\tau)$ is equal to $1 - \tau + \mathcal{O}(\tau^2)$.

Additional differences are in the nature of details. Both of the previous models use a more conventional model for the shell dynamics. They construct a complex angle measuring yaw and pitch and a differential equation containing various moment coefficients. The fluid reaction coefficients are calculated from the fluid dynamic solution. One interesting difference arising from this approach is the fact the existing models predict that the fluid moments should be proportional to τ, while the present model predicts the moments to be proportional to τ^2. [One factor of τ comes from the fact that Γ must vanish when $\tau = 0$ and the second comes from differentiating Eq. (27).]

It can be shown that the side moment coefficient (equivalent to τG_2) calculated using the resonant solution given here goes to zero with τ. The remainder of the solution is sufficiently complicated that such a demonstration has not been found.

A final difference between the present model and the two previous ones is in the method of computation used to generate growth rate vs τ curves. The present model selects the moment of inertia ratio and one moment of inertia and calculates τ and λ. The earlier codes select τ and one moment of inertia and calculate the moment of inertia ratio and λ.

In laboratory gyroscope experiments, a fluid-filled container is spun until the fluid comes to solid corotation with the container and then the spin axis, which had been held fixed during the spin up phase, is released and the gyroscope allowed to cone freely. In a typical experiment, ϵ is small, as is the steady gravitational moment, so that the free coning rate is determined primarily by the moment of inertia ratio of the gyroscope. Thus, to change the coning rate, one changes the moment of inertia ratio. The yaw angle is measured as a

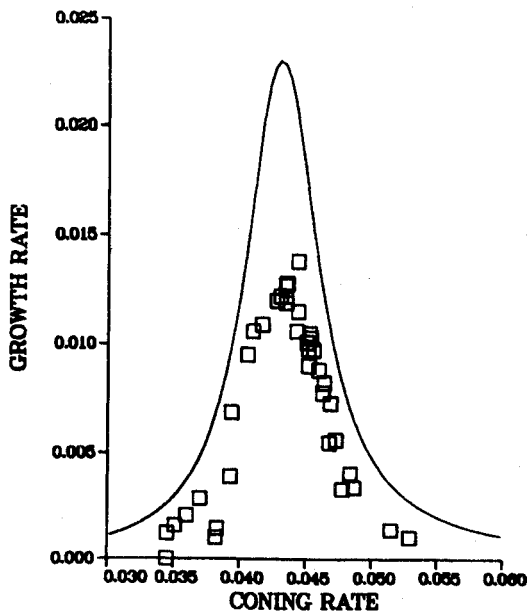

Fig. 1 Growth rate λ vs coning rate τ: $c/a = 3.125$, $E = 1.0 \times 10^{-5}$, $Re = 100{,}000$ (Ref. 9).

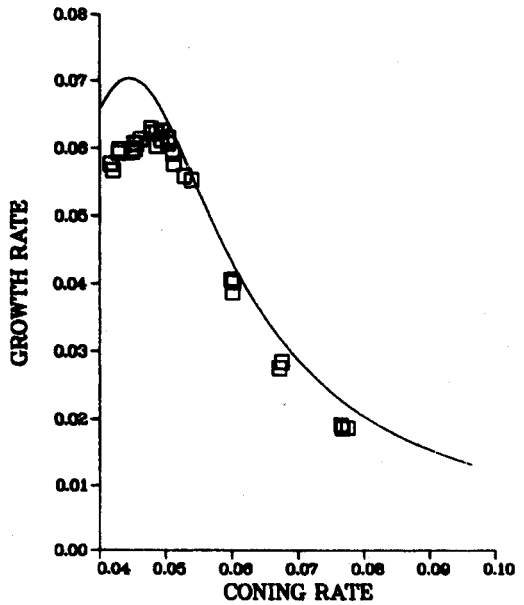

Fig. 2 Growth rate λ vs coning rate τ: $c/a = 1.0415$, $E = 8.1 \times 10^{-5}$, $Re = 12{,}400$ (Ref. 9).

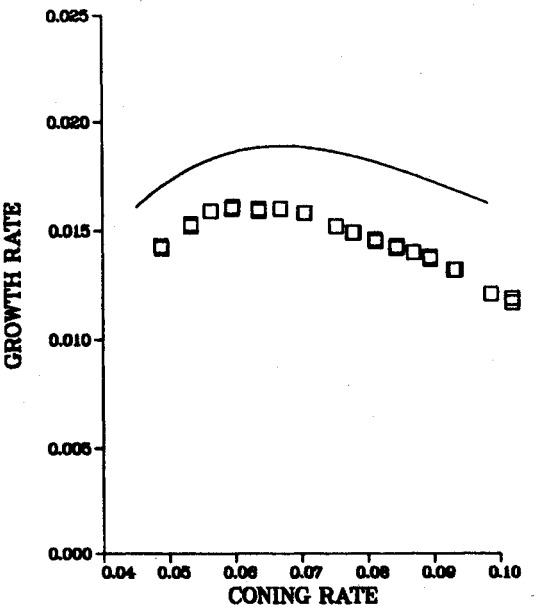

Fig. 4 Growth rate λ vs coning rate τ: $c/a = 1.0415$, $E = 9.5 \times 10^{-4}$, $Re = 1054$ (Ref. 9).

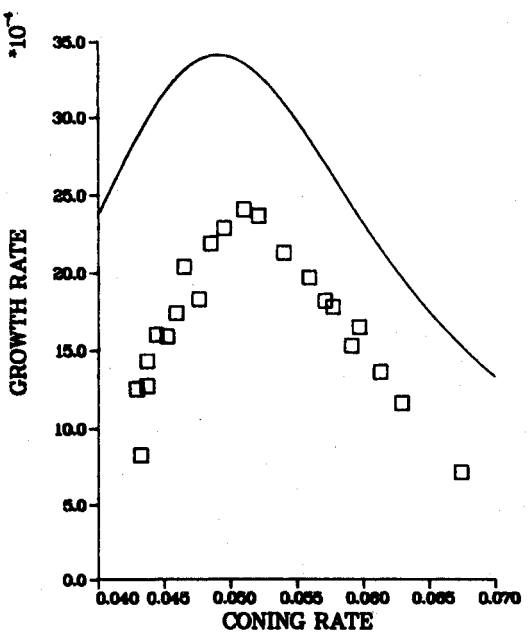

Fig. 3 Growth rate λ vs coning rate τ: $c/a = 3.125$, $E = 2.0 \times 10^{-4}$, $Re = 5000$ (Ref. 9).

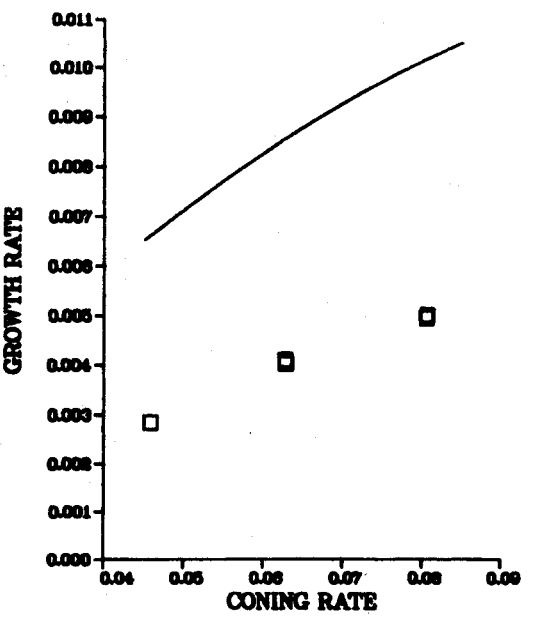

Fig. 5 Growth rate λ vs coning rate τ: $c/a = 1.0415$, $E = 8.9 \times 10^{-3}$, $Re = 112$ (Ref. 9).

function of time, from which one can deduce the coning amplitude and frequency as a function of time. From these one can find the growth rate, $\lambda\tau$ as a function of τ.

The growth rate should be small for the quasistatic assumption to be justified. This translates into the condition that $\lambda\tau \ll E^{1/2}/(c/a)$. Many of the existing experiments do not meet this condition and may not be accurately described by this analysis.

Experiments at the Ballistic Research Lab (BRL) at the Aberdeen Proving Ground prior to 1980 are summarized in Whiting and Gerber.[8] These data are of limited utility because the moment of inertia ratio was altered by changing I_z, which also changed I_x. No record was kept of the latter (although it cannot have changed much, because I_x for these devices is dominated by the nonrotating masses of the gimbals and mounts).

More recent experiments[9] have been made with a fixed I_z and a variable I_x, so that there is a clean separation of the two parameters and the theoretical calculation is straightforward. Figures 1-5 show a representative sample of the experiments from Ref. 9. For these figures the axis labeled growth rate refers to λ, not $\lambda\tau$, and coning rate means τ.

The quasistatic criterion for the data of Figs. 1-5 is that $\lambda\tau$ be small compared to 0.001, 0.009, 0.005, 0.031, and 0.094, respectively. The data of Fig. 1 are marginal with respect to this criterion; the others are probably reasonable.

For a linear theory to be a reasonable approximation, the nondimensional amplitude one calculates should be small compared to unity. That amplitude can be estimated to be less than the forcing amplitude divided by $E^{1/2}$ ($= \alpha\tau/E^{1/2}$). If one asks that $\alpha\tau E^{-1/2}$ be less than 0.1 for one to have confidence in the linear theory, then the maximum α (in radians) admissible

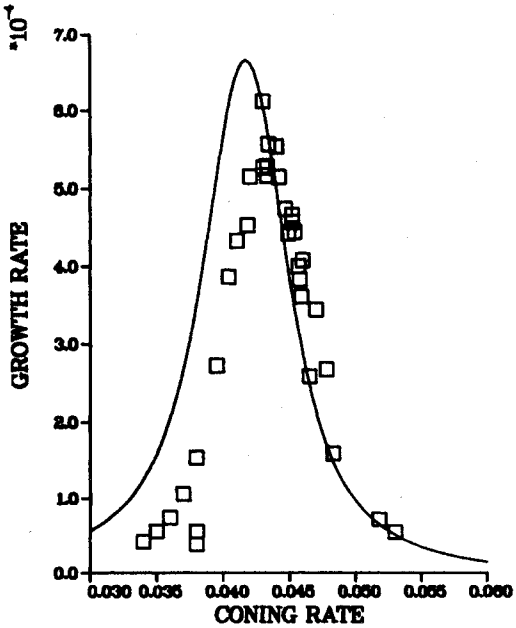

Fig. 6 Growth rate $\lambda\tau$ vs coning rate τ: $E=1.1\times10^{-5}$ (solid line is Murphy calculation).

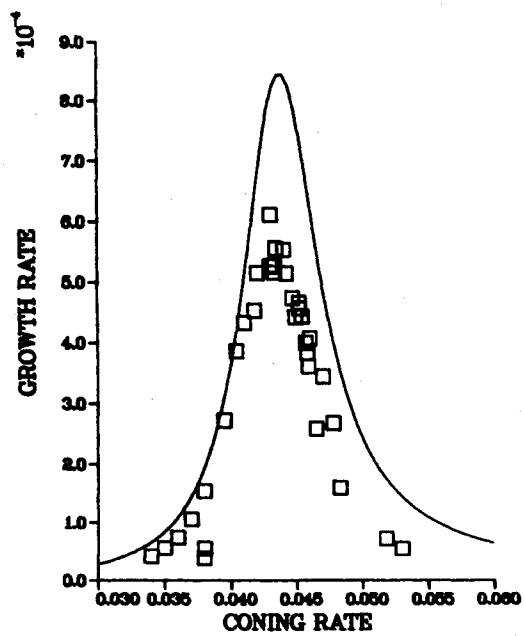

Fig. 7 Growth rate $\lambda\tau$ vs coning rate τ: $E=1.1\times10^{-5}$ (solid line is calculation for the present theory).

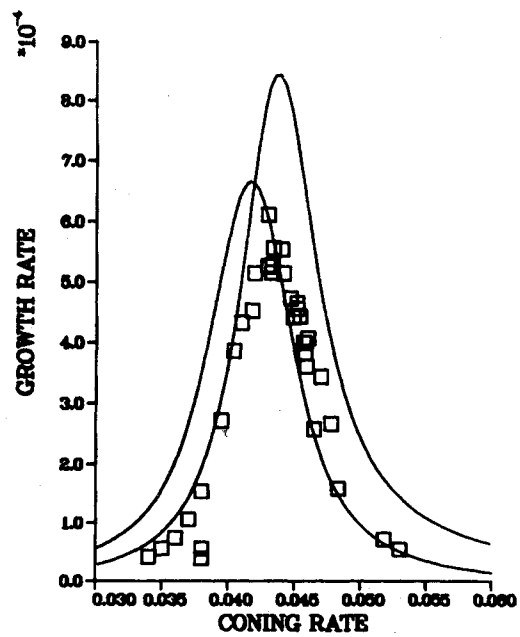

Fig. 8 Growth rate $\lambda\tau$ vs coning rate τ: $E=1.1\times10^{-5}$ (left-hand solid line from Fig. 7, right-hand solid line from Fig. 6).

for the data of Figs. 1-5 are 0.070, 0.180, 0.272, 0.513, and 1.18, respectively. D'Amico (personal communication) has provided the maximum α of the experiments for which growth rates were taken. In no case were these limits exceeded, although it should be remembered that this is only an estimate and if there is a discrepancy at the highest *Re*, it is possible that nonlinear effects could be responsible.

The question of stability of the linear theory is open and well beyond the scope of this paper.

Bearing friction was mentioned in passing above. D'Amico (personal communication) gives estimates of the friction for the cases shown in Figs. 2 and 3. These are in the form of the decay of coning angle for the empty gyroscope. The results are $-\lambda\tau$ equal to approximately 2.5×10^{-5}, giving λ of a few times 10^{-4}. If one adds a number of this size to the data to provide an estimate of the net growth rate, the agreement shown in Fig. 2 is not affected and that of Fig. 3 is improved considerably.

In summary, the data for Fig. 1 probably reflect the beginning of nonlinear or time-dependent phenomena and those of Figs. 2-5 reflect some real agreement between theory and experiment.

A direct comparison of the two analytic approaches is possible for a single experiment (done in the same manner as those reported in Ref. 9) for which predictions from the present work and from the analysis done by Murphy are available. The Ekman number for this experiment is 1.1×10^{-5} and $\epsilon=1.6\times10^{-3}$.

Figures 6-8 show results of this experiment as $\lambda\tau$ vs λ, with theoretical curves generated by the Murphy model (Fig. 6) and the present model (Fig. 7). Both curves are drawn together on Fig. 8 for an easier comparison.

The quasistatic approximation, used in all approaches, requires that $\lambda\tau$ be small compared to 10^{-3}. At the peaks both observed and calculated $\lambda\tau$ approach 10^{-3}, so that the amplitudes of the peaks may be suspicious. The major point of these figures is not the magnitude of the peak response, but the more precise location of the peak in $\lambda\tau$ as a function of τ, supporting the contention that the time transformation given by Eq. (32) is more appropriate than that given by Eq. (33) for gyroscope problems and possibly for projectile problems as well.

Appendix: Details of the Resonant Solution

The resonant velocity components can be written out in terms of the pressure

$$P=J_1(jr)\sin kz \tag{A1}$$

by direct substitution. (The subscript H is to be understood throughout this Appendix.) The result is

$$U=-ik/(2s^2X)\,[(2+s)J_0(jr)+(2-s)J_2(jr)]\sin kz$$

$$V=k/(2s^2X)\,[(2+s)J_0(jr)-(2-s)J_2(jr)]\sin kz$$

$$W=i(k/s)J_1(jr)\cos kz \tag{A2}$$

The use of Bessel function identities and the radial boundary conditions allows one to write down the following useful identities:

$$J_2(j) = (2+s)J_1(j)/(sj), \quad J_0(j) = -(2-s)J_1(j)/(sj) \tag{A3}$$

On the endwalls the boundary-layer equations are those of the periodic Ekman layer and one can write the two tangential components of the boundary-layer velocity as

$$(\tilde{U}+i\tilde{V}) = \pm i(k/s^2X)\sin(kc/a)(2-s)J_2(jr) \times \exp[\pm(1+i)[(2+s)/2E]^{1/2}(z\mp c/a)]$$

$$(\tilde{U}-i\tilde{V}) = \pm i(k/s^2X)\sin(kc/a)(2+s)J_0(jr) \times \exp[\pm(1-i)[(2-s)/2E]^{1/2}(z\mp c/a)] \tag{A4}$$

The associated Ekman suction can be calculated from the divergence condition. That result is

$$\tilde{W} = -(k^2/2s^3X)(E/2)^{1/2}[S^+ - iS^-]\sin(kc/a)J_1(jr) \tag{A5}$$

where S^+ and S^- are defined in the text.

The pressure associated with this boundary layer is $\mathcal{O}(E)$ smaller and is thus negligible for all calculations reported in this work.

The two tangential boundary-layer momentum equations on $r=1$ uncouple. They are of the same form, namely

$$(is - E\partial_r^2)(\tilde{V}, \tilde{W}) = 0 \tag{A6}$$

The boundary-layer components are then given by

$$\tilde{V} = (1/s)J_1(j)\sin kz \exp[(1+i)(s/2E)^{1/2}(r-1)]$$

$$\tilde{W} = -i(k/s)J_1(j)\cos kz \exp[(1+i)(s/2E)^{1/2}(r-1)] \tag{A7}$$

and the Ekman suction is

$$\tilde{U} = -(1+i)(A/s)(1+k^2)(E/2s)^{1/2}J_1(j)\sin kz \tag{A8}$$

The pressure associated with this boundary layer is found from the radial momentum equation, which is, to leading order

$$-2\tilde{V} + \tilde{P}_r = 0 \tag{A9}$$

so that

$$\tilde{P} = 2(1-i)(E/2s^3)^{1/2}J_1(j)\sin kz \tag{A10}$$

on the outer wall.

Acknowledgments

The author wishes to thank the Ballistic Research Laboratory, Launch and Flight Division for hospitality during his stay in Aberdeen, and particularly to thank his host, W. P. D'Amico, for hospitality as well as for providing access to the original data used in assessing the work reported here.

References

[1] Gans, R. F., "On the Precession of a Resonant Cylinder," *Journal of Fluid Mechanics*, Vol. 41, No. 4, 1970, pp. 865-872.

[2] Murphy, C. H., "Angular Motion of a Spinning Projectile with a Viscous Payload," ARBRL-MR-03194, 1982.

[3] Gerber, N., Sedney, R., and Bartos, J. M., "Pressure Moment on a Liquid-Filled Projectile: Solid Body Rotation," ARBRL-TR-02422, 1982.

[4] Gerber, N. and Sedney, R., "Moment on a Liquid-Filled Spinning and Nutating Projectile: Solid Body Rotation," ARBRL-TR-02470, 1983.

[5] Erdelyi, A., Magnus, W., Oberhettinger, F., and Tricomi, F. G., *Higher Transcendental Functions*, Vol. 2, McGraw-Hill Book Co., New York, 1953.

[6] Wedemeyer, E. H., "Viscous Correction to Stewartson's Stability Criterion," BRL Rept. 1325, 1966.

[7] Greenspan, H. P., *The Theory of Rotating Fluids*, Cambridge University Press, Cambridge, England, 1968, Sec. 2.13, pp. 68-78.

[8] Whiting, R. D. and Gerber, N., "Dynamics of a Liquid-Filled Gyroscope: Update of Theory and Experiment," ARBRL-TR-02221, 1980.

[9] D'Amico, W. P. Jr. and Rogers, T. H., "Yaw Instabilities Produced by Rapidly Rotating, Highly Viscous Liquids," AIAA Paper 81-0224, 1981.